Nucleosynthesis in Accretion Flows Around Black Holes

Banibrata Mukhopadhyay and Sandip K. Chakrabarti

S.N. Bose National Centre for Basic Sciences, JD Block, Salt Lake, Sector-III, Calcutta-700091, INDIA

arXiv:astro-ph/9912568v1 31 Dec 1999

Abstract. Significant nucleosynthesis is possible in the centrifugal pressure-supported dense and hot region of the accretion flows which deviate from Keplerian disks around black holes. We compute composition changes and energy generations due to such nuclear processes. We use a network containing 255 species and follow the changes in composition. Highly viscous, high-accretion-rate flows deviate from a Keplerian disk very close to the black hole and the temperature of the flow is very small due to Compton cooling. No significant nucleosynthesis takes place in these cases. Low-viscosity and lower-accretion-rate hot flows deviate farther out and significant changes in composition are possible in these cases. We suggest that such changes in composition could be contributing to the metallicities of the galaxies. Moreover, the radial variation of the energy generation/absorption specifically due to proton capture and photo-dissociation reactions could cause instabilities in the inner regions of the accretion flows. For most of these cases sonic point oscillations may take place. We discuss the possibility of neutrino emissions.

Key words: black hole physics — stars: neutron — accretion, accretion disks —- shock waves – nucleosynthesis

1. Introduction

In Chakrabarti & Mukhopadhyay (1999, hereafter referred to as Paper 1) we studied the result of nucleosynthesis in hot, highly viscous accretion flows with small accretion rates and showed that neutron tori can form around a black hole. In the present paper, we study nucleosynthesis in disks in other parameter space, where the photo-dissociation may not be complete and other reactions may be important, and show that depending on the accretion parameters, abundances of new isotopes may become abnormal around a black hole. Thus, observation of these isotopes may give a possible indication of black holes at the galactic center or in a binary system.

Earlier, Chakrabarti (1986) and Chakrabarti et al.(1987, hereinafter CJA) initiated discussions of nucleosynthesis in sub-Keplerian disks around black holes and concluded that for very low viscosity (α parameter less than around 10^{-4}) and high accretion rates (typically, ten times the Eddington rate) there could be significant nucleosynthesis in thick disks. Radiation-pressure-supported thick accretion flows are cooler and significant nucleosynthesis was not possible unless the residence time of matter inside the accretion disk was made sufficiently high by reducing viscosity. The conclusions of this work were later verified by Arai & Hashimoto (1992) and Hashimoto et al. (1993).

However, the theory of accretion flows which contain a centrifugal-pressure-supported hotter and denser region in the inner part of the accretion disk has been developed more recently (Chakrabarti 1990, hereafter C90 and Chakrabarti 1996, hereafter C96). The improvement in the theoretical understanding can be appreciated by comparing the numerical simulation results done in the eighties (e.g. Hawley et al. 1984, 1985) and in the nineties (e.g. Molteni et al. 1994; Molteni et al. 1996; Ryu et al. 1997). Whereas in the eighties the matching of theory and numerical simulations was poor, the matching of the results obtained recently is close to perfect. It is realized that in a large region of the parameter space, especially for lower accretion rates, the deviated flow would be hot and a significant nuclear reaction is possible without taking resort to very low viscosity.

We arrive at a number of the important conclusions: (a) Significant nucleosynthesis is possible in the accretion flows. Whereas most of the matter of modified composition enters inside the black hole, a fraction may go out through

the winds and will contaminate the surroundings in due course. The metalicity of the galaxies may also be influenced. (b) Generation or absorption of energy due to exothermic and endothermic nuclear reactions could seriously affect the stability of a disk. (c) Hot matter is unable to produce Lithium (^7Li) or Deuterium (D) since when the flow is hot, photo-dissociation (photons partially locally generated and the rest supplied by the nearby Keplerian disk (Shakura & Sunyaev 1973) when the region is optically thin) is enough to dissociate all the elements completely into protons and neutrons. Even when photo-dissociation is turned off (low opacity cases or when the system is fundamentally photon-starved) Li was not found to be produced very much. (d) Most significantly, we show that one does not require a very low viscosity for nucleosynthesis in contrary to the conclusions of the earlier works in thick accretion disk (e.g., CJA).

In Paper 1, we already presented the basic equations which govern accretion flows around a compact object, so we do not present them here. The plan of the present paper is the following: we present a set of solutions of these equations in the next section which would be used for nucleosynthesis work. When nucleosynthesis is insignificant, we compute thermodynamic quantities ignoring nuclear energy generation, otherwise we include it. The detailed method is presented here. We divide all the disks into three categories: ultra-hot, moderately hot, and cold. In Sect. 3, we present the results of nucleosynthesis for these cases. We find that in ultra-hot cases, the matter is completely photo-dissociated. In moderately hot cases, proton-capture processes along with dissociation of deuterium and ^3He are the major processes. In the cold cases, no significant nuclear reactions go on. In Sect. 4, we discuss the stability properties of the accretion disks in presence of nucleosynthesis and conclude that only the very inner edge of the flow is affected. Nucleosynthesis may affect the metallicities of the galaxies as well as Li abundance in companions in black hole binaries. In Sect. 5, we discuss these issues and draw our conclusions.

2. Typical Solutions of Accretion Flows

In our work below, we choose a Schwarzschild black hole and use the Schwarzschild radius $2GM/c^2$ to be the unit of the length scale where G and c are the gravitational constant and the velocity of light respectively. We choose c to be the unit of velocity. We also choose the cgs unit when we find it convenient to do so. The nucleosynthesis work is done using cgs units and the energy release rates are in that unit as well.

A black hole accretion disk must, by definition, have *radial* motion, and it must also be transonic, i.e., matter must be supersonic (C90) while entering through the horizon. The supersonic flow must be sub-Keplerian and therefore deviate from the Keplerian disk away from the black hole. The location where the flow may deviate will depend on the cooling and heating processes (which depend on viscosity). Several solutions of the governing equations (see Eq. 2(a-d) of Paper 1) are given in C96. By and large, we follow this paper to compute thermodynamical parameters along a flow. However, we have considered Comptonization as in Chakrabarti & Titarchuk (1995, hereafter CT95) and Chakrabarti (1997, hereafter C97). Due to computational constraints, we include energy generation due to nuclear reactions (Q_{nuc}) only when it is necessary (namely, when $|Q_{\mathrm{nuc}}|$ is comparable to energy generation due to viscous effects), and we do not consider energy generation due to magnetic dissipation (due to reconnection effects, for instance). In Fig. 1, we show a series of solutions which we employ to study nucleosynthesis processes. We plot the ratio λ/λ_K (Here, λ and λ_K are the specific angular momentum of the disk and the Keplerian angular momentum respectively.) as a function of the logarithmic radial distance. The coefficient of the viscosity parameters are marked on each curve. The other parameters of the solution are in Table 1. These solutions are obtained with constant $f = 1 - Q^-/Q^+$ and Q^+ include only the viscous heating. In presence of significant nucleosynthesis, the solutions are obtained by choosing $f = 1 - Q^-/(Q^+ + Q_{\mathrm{nuc}})$, where Q_{nuc} is the net energy generation or absorption due to exothermic and endothermic reactions. The motivation for choosing the particular cases are mentioned in the next section. At $x = x_K$, the ratio $\lambda/\lambda_K = 1$ and therefore x_K represents the transition region where the flow deviates from a Keplerian disk. First, note that when other parameters (basically, specific angular momentum and the location of the inner sonic point) remain roughly the same, x_K changes inversely with viscosity parameter α_Π (C96). (The only exception is the curve marked with 0.01. This is because it is drawn for $\gamma = 5/3$; all other curves are for $\gamma = 4/3$.) If one assumes, as Chakrabarti & Titarchuk (1995) and Chakrabarti (1997) did, that the alpha viscosity parameter *decreases* with vertical height, then it is clear from the general behaviour of Fig. 1 that x_K would go up with height. The disk will then look like a sandwich with higher viscosity Keplerian matter flowing along the equatorial plane. As the viscosity changes, the sub-Keplerian and Keplerian flows redistribute (Chakrabarti & Molteni 1995) and the inner edge of the Keplerian component also recedes or advances. This fact that the inner edge of the disk should move in and out when the black hole goes into soft or hard state (as observed by, e.g., Gilfanov et al. 1997; Zhang et al. 1997) is thus naturally established from this disk solution.

In C90 and C96, it was pointed out that in a large region of the parameter space, especially for intermediate viscosities, centrifugal-pressure-supported shocks would be present in the hot, accretion flows. In these cases a shock-
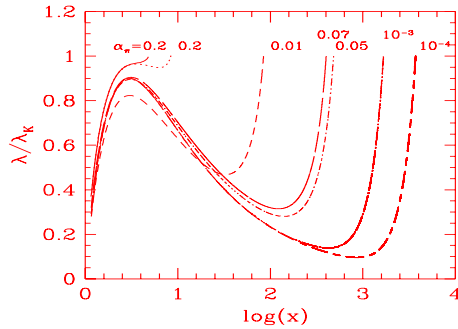
Fig. 1. Variation of λ/λ_K with logarithmic radial distance for a few solutions which are employed to study nucleosynthesis. The viscosity parameter α_Π is marked on each curve. $x = x_K$ where $\lambda/\lambda_K = 1$, represents the location where the flow deviates from a Keplerian disk. Note that except for the dashed curve marked 0.01 (which is for $\gamma = 5/3$, and the rest are for $\gamma = 4/3$), x_K generally rises with decreasing α_Π. Thus, high viscosity flows must deviate from the Keplerian disk closer to the black hole.

free solution passing through the outer sonic point was present. However, this branch is not selected by the flow and the flow passes through the higher entropy solution through shocks and the inner sonic points instead. This assertion has been repeatedly verified independently by both theoretical (Yang & Kafatos 1995, Nobuta & Hanawa 1994; Lu & Yuan 1997; Lu et al. 1997) and numerical simulations (with independent codes, Chakrabarti & Molteni 1993; Sponholz & Molteni 1994; Ryu et al. 1995, Molteni et al. 1996 and references therein). When the shock forms, the temperature of the flow suddenly rises and the flow slows down considerably, raising the residence time of matter significantly. This effect of shock-induced nucleosynthesis is also studied in the next section and, for comparison, the changes in composition in the shock-free branch were also computed, although it is understood that the shock-free branch is unstable. Our emphasis is not on shocks per se, but on the centrifugal-pressure-dominated region where the accreting matter slows down. When the shock does not form, the rise in temperature is more gradual. We generally follow the results of CT95 and C97 to compute the temperature of the Comptonized flow in the sub-Keplerian region which may or may not have shocks. Basically we borrow the mean factor $F_{\mathrm{Compt}} \lesssim 1$ by which the temperature of the flow at a given radius x ($< x_K$) is reduced due to Comptonization process from the value dictated by the single-temperature hydrodynamic equations. This factor is typically $1/30 \sim 0.03$ for very low ($\lesssim 0.1$) mass accretion rate of the *Keplerian component* (which supplies the soft photons for the Comptonization) and around $1/100 \sim 0.01$ or less for higher Keplerian accretion rates. In presence of magnetic fields, some dissipation is present due to reconnections. Its expression is $Q_{\mathrm{mag}} = \frac{3B^2}{16\pi x \rho} v$ (Shvartsman 1971; Shapiro 1973). We do not assume this heating in this paper.

The list of major nuclear reactions such as PP chain, CNO cycle, rapid proton capture and alpha (α) processes, photo-dissociation etc. which may take place inside a disk are already given in CJA, and we do not repeat them here. Suffice it to say that due to the hotter nature of the sub-Keplerian disks, especially when the accretion rate is low and Compton cooling is negligible, the major process of hydrogen burning is some rapid proton capture process (which operates at $T \gtrsim 0.5 \times 10^9$K) and mostly (p, α) reactions as opposed to the PP chain (which operates at much lower temperature $T \sim 0.01 - 0.2 \times 10^9$K) and CNO cycle (which operates at $T \sim 0.02 - 0.5 \times 10^9$K) as in CJA.

Typically, accretion onto a stellar-mass black hole takes place from a binary companion which could be a main sequence star. In a supermassive black hole at a galactic center, matter is presumably supplied by a number of nearby

stars. Because it is difficult to establish the initial composition of the inflow, we generally take the solar abundance as the abundance of the Keplerian disk. Furthermore, the Keplerian disk being cooler, and the residence time inside it being insignificant compared to the hydrogen burning time scale, we assume that for $x \gtrsim x_K$, the composition of the gas remains the same as that of the companion star, namely, solar. Thus our computation starts only from the time when matter is launched from the Keplerian disk. Occasionally, for comparison, we run the models with an initial abundance same as the output of big-bang nucleosynthesis (hereafter referred to as 'big-bang abundance'). These cases are particularly relevant for nucleosynthesis around proto-galactic cores and the early phase of star formations. We have also tested our code with an initial abundance same as the composition of late-type stars since in certain cases they are believed to be companions of galactic black hole candidates (Martin et al. 1992, 1994; Filippenko et al. 1995; Harlaftis et al. 1996).

2.1. Selection of Models

In selecting models for which the nucleosynthesis should be studied, the following considerations were made. According to CT95, and C97, there are two essential components of a disk. One is Keplerian (of rate $\dot{m}_d$) and the other is sub-Keplerian halo (of rate $\dot{m}_h$). For $\dot{m}_d \lesssim 0.1$ and $\dot{m}_h \lesssim 1$, the black hole remains in hard states. A lower Keplerian accretion rate *generally* implies a lower viscosity and a larger x_K ($x_K \sim 30-1000$; see, C96 and C97). In this parameter range the protons remain hot, typically, $T_p \sim 1 - 10 \times 10^9$ degrees or so. This is because the efficiency of emission is lower ($f = 1 - Q^-/Q^+ \sim 0.1$, where, Q^+ and Q^- are the height-integrated heat generation and heat loss rates [ergs cm^{-2} sec^{-1}] respectively. Also, see Rees (1984), where it is argued that $\dot{m}/\alpha^2$ is a good indication of the cooling efficiency of the hot flow.). Thus, we study a group of cases (Group A) where the net accretion rate $\dot{m} \sim 1.0$ and the viscosity parameter $\alpha \sim 0.001-0.1$. The Comptonization factor $F_{\mathrm{Compt}} \sim 0.03$, i.e., the cooling due to Comptonization reduces the mean temperature roughly by a factor of around 30, which is quite reasonable. Here, although the density of the gas is low, the temperature is high enough to cause significant nuclear reactions in the disk.

When the net accretion rate is very low ($\dot{m} \lesssim 0.01$) such as in a quiescence state of an X-ray novae, the dearth of soft photons keeps the temperature of the sub-Keplerian flow to a very high value and a high Comptonization factor $F_{\mathrm{Compt}} \sim 0.1$ could be used (Group B). Here significant nuclear reaction takes place, even though the density of matter is very low. Basically, the entire amount of matter is photo-dissociated into protons and neutrons in this case even when opacity is very low.

In the event the inflow consist of both the Keplerian (accretion rate $\dot{m}_d$) and sub-Keplerian (accretion rate $\dot{m}_h$) matter as the modern theory predicts, there would be situations where the *net* accretion rate is high, say $\dot{m} = \dot{m}_d + \dot{m}_h \sim 1 - 5$, and yet the gas temperature is very high ($T > 10^9$). This happens when viscosity is low to convert sub-Keplerian inflow into a Keplerian disk. Here, most of the inflow is in the sub-Keplerian component and very little ($\dot{m}_d \sim 0.01$) matter is in the Keplerian flow. Dearth of soft photons keeps the disk hot, while the density of reactants is still high enough to have profuse nuclear reactions. The simple criteria for the cooling efficiency (that $\dot{m}/\alpha^2 > 1$ would cool the disk, see Rees 1984) will not hold since the radiation source (Keplerian disk) is different from the cooling body (sub-Keplerian disk).

One could envisage yet another set of cases (Group C), where the accretion rate is very high ($\dot{m} \sim 10 - 100$), and the soft photons are so profuse that the sub-Keplerian region of the disks becomes very cold. In this case, typically, viscosity is very high 0.2, x_K becomes low ($x_K \sim 3 - 10$). The efficiency of cooling is very high ($Q^+ \approx Q^-$, i.e., $f \approx 0$). The Comptonization factor is low $F_{\mathrm{Compt}} \lesssim 0.01$. The black hole is in a soft state. There is no significant nuclear reaction in these cases. In the proto-galactic phase when the supply of matter is *very* high, while the viscosity may be so low (say, 10^{-4}) that the entire amount is not accreted, one can have an ultra-cold accretion flow with $F_{\mathrm{Compt}} \sim 10^{-3}$. In this case also not much nuclear reaction goes on.

The above simulations have been carried out with polytropic index $\gamma = 4/3$. In reality, the polytropic index could be in between $4/3$ and $5/3$. If $\gamma < 1.5$ then shocks would form as in some of the above cases. However, for $\gamma > 1.5$, standing shocks would not form (C96). We have included one illustrative example of a shock-free case with $\gamma = 5/3$ which is very hot and we have presented the result in Group B. In this case the Keplerian component is far away and the intercepted soft photons are very few.

2.2. Selection of the Reaction Network

In selecting the reaction network we kept in mind the fact that hotter flows may produce heavier elements through triple-α and proton and α capture processes. Similarly, due to photo-dissociation, significant neutrons may be produced. Thus, we consider a sufficient number of isotopes on either side of the stability line. The network thus contains protons, neutrons, till ^{72}Ge – altogether 255 nuclear species. The network of coupled non-linear differential equation is linearized

and evolved in time along the solution of C96 obtained from a given set of initial parameters of the flow. This well proven method is widely used in the literature (see Arnett & Truran 1969; Woosley et al. 1973).

The reaction rates were taken from Fowler et al. (1975) including updates by Harris et al. (1983). Other relevant references from where rates have been updated are: Thielemann (1980); Wallace & Woosley (1981); Wagoner et al.(1967); Fuller et al.(1980, 1982). For details of the procedure of adopting reaction rates, see, CJA and Jin et al.(1989, hereinafter JAC). The solar abundance which was used as the initial composition of the inflow was taken from Anders & Ebihara (1982).

3. Results

In this section, we present a few major results of our simulations using different parameter groups as described above. For a complete solution of the sub-Keplerian disks (C96) we need to provide (a) the mass of the black hole M, (b) the viscosity parameter α_Π, (c) the cooling efficiency factor f, (d) the Comptonization factor F_{Compt}, (d) the net accretion rate of the flow $\dot{m}$, (e) the inner sonic point location x_{in} through which the flow must pass and finally, (f) the specific angular momentum λ_{in} at the inner sonic point.

The following table gives the cases we discuss in this paper. The Π-stress viscosity parameter α_Π, the location of the inner sonic point x_{in} and the value of the specific angular momentum at that point λ_{in} are free parameters. The net accretion rate $\dot{m}$, the Comptonization factor F_{Compt} and the cooling efficiency f are related quantities (CT96, C97). For extremely inefficient cooling, $f \sim 1.0$, and for extremely efficient cooling $f = 0$ or even negative. The derived quantities, such as the value of maximum temperature T_9^{max} of the flow (in units of 10^9K), density of matter (in cgs units) at T_9^{max}, x_K, the location from where the Keplerian disk on the equatorial plane becomes sub-Keplerian are also provided in the table. In the rightmost column, we present whether the inner edge of the disk is stable (S) or unstable (U) in the presence of the accretion flow. Three groups are separated as the parameters are clearly from three distinct regimes.

TABLE 1

Model	$M/M_\odot$	γ	x_{in}	λ_{in}	α_Π	$\dot{m}$	f	F_{Compt}	x_K	T_9^{max}	ρ_{max}	S/U
A.1	10	4/3	2.7945	1.65	0.001	1	0.1	0.03	1655.7	5.7	6.2×10^{-7}	S
A.2	10	4/3	2.9115	1.6	0.07	1	0.1	0.03	401.0	4.7	4.9×10^{-7}	S
A.3	10^6	4/3	2.9115	1.6	0.07	1	0.1	0.03	401.0	4.7	4.9×10^{-12}	U
B.1	10	4/3	2.8695	1.6	0.05	0.01	0.5	0.1	481.4	16.5	3.9×10^{-9}	S
B.2	10	4/3	2.8695	1.6	0.05	4	0.5	0.1	481.4	16.5	1.6×10^{-8}	U
B.3	10	5/3	2.4	1.5	0.01	0.001	0.5	0.1	84.4	47	3.3×10^{-10}	S
B.4	10	4/3	2.795	1.65	0.2	0.01	0.2	0.1	8.4	13	1.1×10^{-8}	S
C.1	10	4/3	2.795	1.65	0.2	100	0.0	0.01	4.8	0.8	1.1×10^{-4}	S
C.2	10^6	4/3	2.795	1.65	10^{-4}	100	0.0	0.001	3657.9	0.2	6.2×10^{-10}	S

The basis of our three groupings are clear from the Table. Very low $\dot{m}/\alpha_\Pi^2$ in Group B makes the cooling efficiency to be very small. Thus we choose a relatively large $f \sim 0.2 - 0.5$. It also makes the cooling due to Comptonization to be very low ($F_{\mathrm{Compt}} \sim 0.1$). Thus the disks could be ultra-hot. Intermediate $\dot{m}/\alpha_\Pi^2$ in Group A means that the efficiency of cooling is intermediate $f \sim 0.1$ and the Compton cooling of the sub-Keplerian region is average: $F_{\mathrm{Compt}} \sim 0.03$. The sub-Keplerian disk in this case is neither too hot nor too cold. Extremely high $\dot{m}/\alpha_\Pi^2$ causes a strong cooling in Group C. Thus, we choose $f = 0$, and a very efficient Compton cooling $F_{\mathrm{Compt}} \sim 0.01 - 0.001$. As a result, the disk is also very cold. Now, we present our numerical results in these cases.

3.1. Nucleosynthesis in Moderately Hot Flows

Case A.1: In this case, the termination of the Keplerian component in the weakly viscous flow takes place at $x = 1655.7$. The soft photons intercepted by the sub-Keplerian region reduce the temperature of this region but not by a large factor. The net accretion rate $\dot{m} = 1$ is the sum of (very low) Keplerian component and the sub-Keplerian component. Using computations of CT95 and C97 for $\dot{m}_d \sim 0.1$ and $\dot{m}_h \sim 0.9$, we find that the electron temperature T_e is around 60keV $T9 \sim 0.6$ (T_9 is the temperature in units of 10^9K) and the ion temperature is around $T_9 = 2.5$. This fixes the Comptonization factor to about $F_{Compt} = 0.03$. This factor is used to reduce the temperature distribution of solutions of C96 (which does not explicitly use Comptonization) to temperature distribution *with* Comptonization. The ion temperature (in T_9) and density (in units of 10^{-10} gm cm^{-3} to bring in the same plot) distribution computed

in this manner are shown in Fig. 2a. Figure 2b gives the velocity distribution (velocity is measured in units of 10^{10} cm sec^{-1}). Note the sudden rise in temperature and slowing down of matter close to the centrifugal barrier $x \sim 30$. Figure 2c shows the changes in composition as matter is accreted onto the black hole. Only those species with abundance $Y_i \gtrsim 10^{-4}$ have been shown for clarity. Also, compositions closer to the black hole are shown, as variations farther out are negligible. Most of the burning of species takes place below $x = 10$. A significant amount of the neutrons (with a final abundance of $Y_n \sim 10^{-3}$) is produced by the photo-dissociation process. Note that closer to the black hole, ^{12}C, ^{16}O, ^{24}Mg and ^{28}Si are all destroyed completely, even though at around $x = 5$ or so, the abundance of some of them went up first before going down. Among the new species which are formed closer to the black hole are ^{30}Si, ^{46}Ti, ^{50}Cr. The final abundance of ^{20}Ne is significantly higher than the initial value. This was not dissociated as the residence time in hotter region was insufficient. Thus a significant metalicity could be supplied by winds from the centrifugal barrier.

Fig. 2a
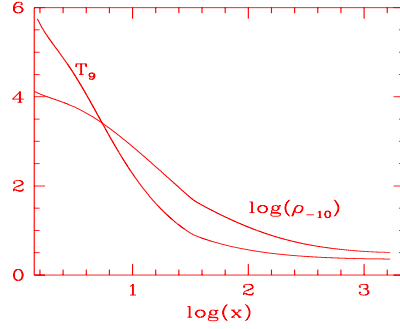
Fig. 2b
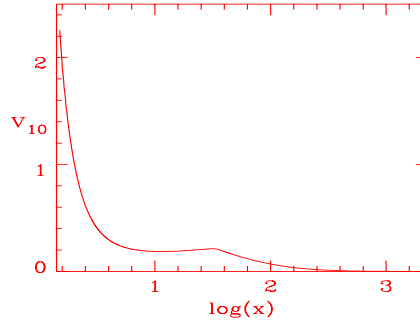
Fig. 2c
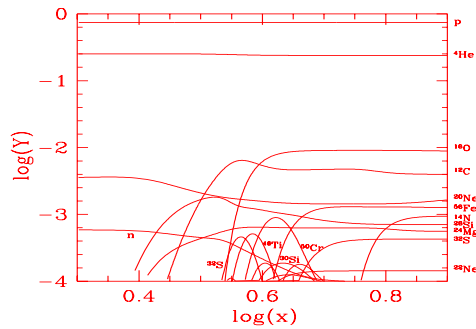
Figure 2d shows the energy release and absorption due to exothermic and endothermic nuclear reactions (Q_{nuc}) that are taking place inside the disk (solid). Superposed on it are the energy generation rate Q^+ (long dashed curve) due to viscous process and the energy loss rate Q^- in the sub-Keplerian flows. For comparison, we also plot the hypothetical energy generation and loss rates (short dashed curves marked as Q^+_{Kep} and Q^-_{Kep} respectively) if the disk had purely Keplerian angular momentum distribution even in the sub-Keplerian regime. All these quantities are in units of 3×10^6 and they represent height-integrated energy release rate (ergs cm^{-2} sec^{-1}). Note that these Qs are in logarithmic scale (if $Q < 0$, $-log(|Q|)$ is plotted). As matter leaves the Keplerian flow, the proton capture
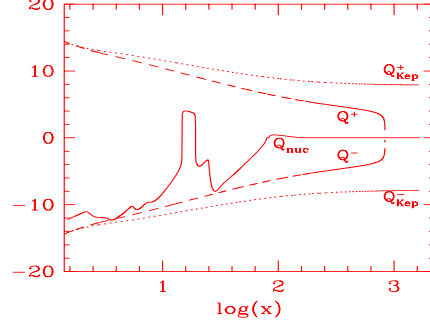
Fig. 2d

Fig. 2. Variation of (a) ion temperature (T_9) and density (ρ_{-10}), (b) radial velocity v_{10}, (c) matter abundance Y_i in logarithmic scale and (d) various forms of height-integrated specific energy release and absorption rates (in ergs cm^{-2} sec^{-1}) when the model parameters are $M = 10 M_\odot$, $\dot{m} = 1.0$, $\alpha_\Pi = 0.001$ as functions of logarithmic radial distance (x in units of Schwarzschild radius). Q is in logarithmic scale. See text and Table 1 for other parameters of Case A.1 which is considered here. The centrifugal barrier slows down and heats up matter where a significant change in abundance takes place ($\Delta Y_i \sim 10^{-3}$).

(p, α) processes (such as $^{18}O(p, \alpha)^{15}N$, $^{15}N(p, \alpha)^{12}C$, $^6Li(p, \alpha)^3He$, $^7Li(p, \alpha)^4He$, $^{11}B(p, \gamma)3\alpha$, $^{17}O(p, \alpha)^{14}N$, etc.) burn hydrogen and release energy to the disk. (Since the temperature of the disk is very high, PP chains or CNO cycles are not the dominant processes for the energy release.) At around $x = 40$, the deuterium starts burning ($D(\gamma, n)p$) and the endothermic reaction causes the nuclear energy release to become 'negative', i.e., a huge amount of energy is absorbed from the disk. At the completion of the deuterium burning (at around $x = 20$) the energy release tends to goes back to the positive value to the level dictated by the original proton capture processes. Excessive temperature at around $x = 5$ breaks ^3He down into deuterium ($^3He(\gamma, p)D$, $D(\gamma, n)p$). Another major endothermic reaction which is dominant in this region is $^{17}O(\gamma, n)^{16}O$. These reactions absorb a significant amount of energy from the flow. Note that the nuclear energy release or absorption is of the same order as the energy release due to viscous process. This energy was incorporated in computing thermodynamic quantities following these steps:
(a) Compute thermodynamic quantities without nuclear energy (b) Run nucleosynthesis code and compute Q_{nuc}
(c) Fit Q_{nuc} using piecewise analytical curves and include this into the definition of f,

$$f = 1 - \frac{Q^-}{Q^+ + Q_{\mathrm{nuc}}} \tag{1}$$

(d) Do sonic point analysis once more using this extra heating/cooling term and compute thermodynamic quantities.
(e) Repeat from step (b) till the results converge. In this case, there in virtually no difference in the solution and the solution appear to be completely stable under nucleosynthesis.

Case A.2: Here we choose the same net accretion rate, but with a larger viscosity. As a result, the Keplerian component moves closer. The Comptonization is still not very effective, and the flow is moderately hot as above with $F_{\mathrm{Compt}} = 0.03$. The flow deviates from a very hot (sufficient to cause the flow to pass through the outer sonic point) Keplerian disk at $x_K = 401.0$, and after passing through an outer sonic point at $x = 50$, and through a shock at $x_S = 15$, the flow enters into the black hole through the inner sonic point at $x = 2.9115$. We show the results both for the shock-free branch (i.e., the one which passes through only the outer sonic point before plunging into the black hole, dotted curves) and the shocked branch of the solution (solid curves). Figure 3a shows the comparison of the temperatures and densities (scaled in the same way as in Fig. 2a). The temperature and density jump sharply at the shock. Figure 3b shows the comparison of the radial velocities. The velocity sharply drops at the shock. Both of these effects hasten the nuclear burning in the case which includes the shock. Figure 3c shows the comparison of the abundances of only those species whose abundances reached a value of at least 10^{-4}. The difference between the shocked and the shock-free cases is that in the shock case similar burning takes place farther away from the black hole because of much higher temperature in the post-shock region.
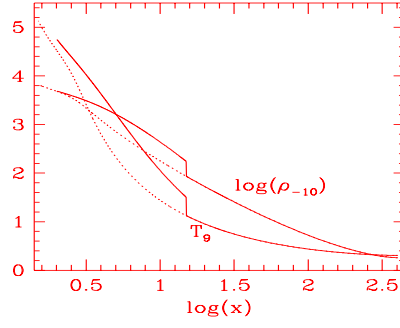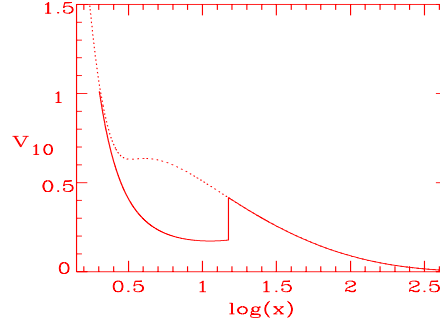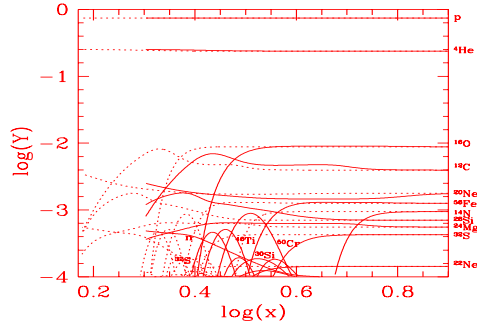
Fig. 3a

Fig. 3b
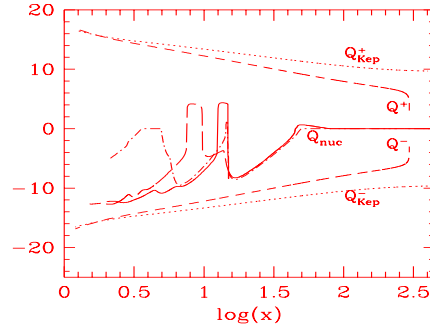

Fig. 3c

Fig. 3d

Fig. 3.: Variation of (a) ion temperature (T_9) and density (ρ_{-10}), (b) radial velocity v_{10}, (c) matter abundance Y_i in logarithmic scale and (d) various forms of specific energy release and absorption rates when the model parameters are $M = 10 M_\odot$, $\dot{m} = 1.0$, $\alpha_\Pi = 0.07$ as functions of logarithmic radial distance (x in units of Schwarzschild radius). See text and Table 1 for other parameters of Case A.2 which is considered here. Solutions in the stable branch with shocks are solid curves and those without the shock are dotted in (a-c). Curves in (d) are described in the text. At the shock temperature and density rise significantly and cause a significant change in abundance even farther out. Shock-induced winds may cause substantial contamination of the galactic composition when parameters are chosen from these regions.

The nature of the (height integrated) nuclear energy release is very similar to Case A.1 as the major reactions which take place inside the disk are basically same, except that the exact locations where any particular reactions take place are different since they are temperature sensitive. In Fig. 3d, we show all the energy release/absorption components for the shocked flow (solid curve). For comparison, we include the nuclear energy curve of the shock-free branch (very long dashed curve). Note that in the post-shock region, hotter and denser flow of the shocked-branch causes a particular nuclear reaction to take place farther away from a black hole when compared with the behaviour in the shock-free branch as is also reflected in the composition variation in Fig. 3c. The viscous energy generation (Q^+) and the loss of energy (Q^-) from the disk (long dashed) and shown. As before, these quantities, if the inner part had Keplerian distribution, are also plotted (short dashed). When big-bang abundance is chosen to be the initial abundance, the net composition does not change very much, but the dominating reactions themselves are somewhat different because the initial compositions are different. The dot-dashed curve shows the energy release/absorption in the shocked flow when big-bang abundance is chosen. All these quantities are, as before, in units of 3×10^6 and they represent height integrated energy release rate (ergs cm^{-2} sec^{-1}). For instance, in place of proton capture reactions for computations with solar abundance, the fusion of deuterium into ^4He plays a dominant role via the following reactions: $D(D,n)^3He$, $D(p,\gamma)^3He$, $D(D,p)T$, $^3He(D,p)^4He$. This is because no heavy elements were present to begin with and proton capture processes involving heavy elements such as were prevalent in the solar abundance case cannot take place here. Endothermic reactions at around $x = 20 - 40$ are dominated by deuterium dissociation as before. However, after the complete destruction of deuterium, the exothermic reaction is momentarily dominated by neutron capture processes (due to the same neutrons which are produced earlier via $D(\gamma,n)p$) such as $^3He(n,p)T$ which produces the spike at around $x = 14.5$. Following this, ^3He and T are destroyed as in the solar abundance case (i.e., $^3He(\gamma,p)D$, $D(\gamma,n)p$, $T(\gamma,n)D$) and reaches the minimum in the energy release curve at around $x = 6$. The tendency of going back to the exothermic region is stopped due to the photo-dissociation of ^4He via $^4He(\gamma,p)T$ and $^4He(\gamma,n)^3He$. At the end of the big-bang abundance calculation, a significant amount of neutrons are produced. The disk was found to be perfectly stable under nuclear reactions.

Case A.3: This case is exactly same as A.2 except that the mass of the black hole is chosen to be $10^6 M_\odot$. The temperature and velocity variations are similar to the above case. Because the accretion rate (in non-dimensional units) is the same, the density (which goes as $\dot{m}/r^2v$) is lower by a factor of 10^{-5}. Tenuous plasma should change its composition significantly only at higher temperatures than in the previous case. However, the increase in residence time by a factor of around 10^5 causes the nuclear burning to take place farther out even at a lower temperature. This is exactly what is seen. Figure 4a shows the comparison (without including nuclear energy) of the composition of matter when the flow has a shock (solid curves) and when the flow is shock-free (dashed curve). We recall that the shock-free flow is in reality not stable. It is kept only for comparison purposes. Note that unlike earlier cases, a longer residence time also causes to burn all the ^{20}Ne that was generated from ^{16}O.
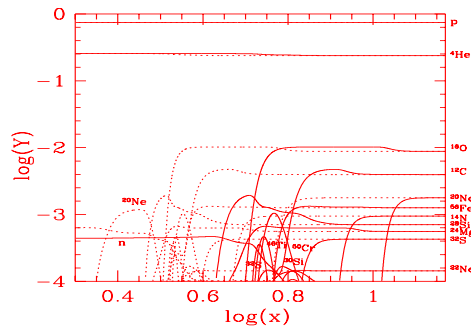

Fig. 4a

In Fig. 4b, we show a comparison of various height-integrated energy release and absorption curves as in Fig. 3d (in ergs cm^{-2} sec^{-1}). The nuclear energy remains negligibly small till around $x = 100$. After that the endothermic reactions dominate. This is due to the dissociation of D, ^3He and ^7Li and also of ^{12}C, ^{16}O, ^{20}Ne etc. all of which produce ^4He. The solid curve is for the branch with a shock and the very long dashed curve is for the shock-free branch. A small amount of neutrons are produced ($Y_n \sim 10^{-3}$) primarily due to the dissociation of D. These considerations are valid for solar abundance as the initial composition. In the case of big-bang abundance (dash-dotted curve), similar
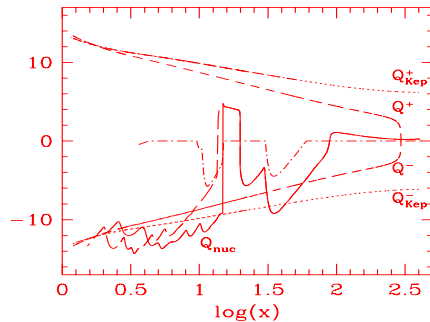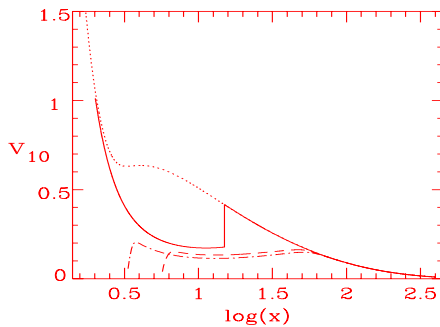
Fig. 4b

Fig. 4c

Fig. 4.: Variation of (a) matter abundance Y_i in logarithmic scale, (b) various forms of height-integrated specific energy release and absorption rates and (c) velocity (in units of 10^{10} cm s^{-1}) when the model parameters are $M = 10^6 M_\odot$, $\dot{m} = 1.0$, $\alpha_{\Pi} = 0.07$ as functions of logarithmic radial distance (x in units of Schwarzschild radius). See text and Table 1 for other parameters of Case A.3. In (a) solutions in the stable branch with shocks are solid curves and those without the shock are short dashed. Curves in (b) are described in the text. Basic conclusions are as in the previous case. In (c), dot-dashed curve and dashed curves are drawn when nuclear energy is taken into account.

reactions take place but no elements heavier than ^7Li are involved. The three successive dips are due to dissociation of D, ^3He and ^4He respectively.

Below $x = 10$, $|Q_{\mathrm{nuc}}|$ is larger compared to Q^+ by 3-4 orders of magnitude. This is because of the superposition of a large number of photo-dissociation effects. We expect that in this case the disk would be unstable. This is exactly what we see. In Fig. 4c, we show the effects of nuclear reactions more clearly. The dotted curve and the solid curves are, as in Fig. 3b, the variation of velocity for the solution without and with shocks, respectively. The dot-dashed curve represents velocity variation without shock when nuclear reaction is included. The dashed curve is the corresponding solution when nucleosynthesis of the shocked branch is included. Both branches are unstable since the steady flow is subsonic at the inner edge. In these cases, the flow is expected to pass through the inner sonic point in a time-dependent manner and some sort of quasi-periodic oscillations cannot be ruled out.

3.2. Nucleosynthesis in Hot Flows

Case B.1: This case is chosen with such a set of parameters that a standing shock forms at $x_s = 13.9$. A very low accretion rate is chosen so that the Compton cooling is negligible and the flow remains very hot (Comptonization factor $F_{\mathrm{Compt}} = 0.1$). We show the results both for the shock-free branch (dashed) and the shocked branch (solid) of

the solution. Figure 5a shows the comparison of the temperatures and densities (in units of 10^{-20} gm cm^{-3} to bring in the same plot). Figure 5b shows the comparison of the radial velocities. This behaviour is similar to that shown in Case A.2. Because the temperature is suitable for photo-dissociation, we chose a very small set of species in the network (only 21 species up to ^{11}B are chosen). Figure 5c shows the comparison of the abundances of proton (p), ^{4}He and neutron (n). In the absence of the shock, the breaking up of ^{4}He into n and p takes place much closer to the black hole, while the shock hastens it due to higher temperature and density. Although initially the flow starts with $Y_p = 0.7425$ and $^{4}He = 0.2380$, at the end of the simulation, only proton ($Y_p \sim 0.8786$) and neutron ($Y_n \sim 0.1214$) remain and the rest of the species become insignificant.

Figure 5d shows the comparison of the height-integrated nuclear energy release (units are as Fig. 2d). As the flow leaves the Keplerian disk at $x_K = 481.4$, the deuterium and ^{9}Be are burnt instantaneously at the cost of some energy from the disk. At the end of deuterium burning at around $x = 200$, the rp and proton capture processes (mainly via $^{11}B(p,\gamma)3^{4}He$ which releases significant energy) and neutron capture ($^{3}He(n,p)T$) take place, but further in, ^{3}He (via $^{3}He(\gamma,p)D$) first and ^{4}He (mainly via $^{4}He(\gamma,n)^{3}He$ and $^{4}He(\gamma,p)T$, $T(\gamma,n)D$) subsequently, are rapidly dissociated. As soon as the entire helium is burnt out, the energy release becomes negligible. This is because there is nothing left other than free protons and neutrons and hence no more reactions take place and no energy is released or absorbed. The solid curve is for the branch with a shock and the very long dashed curve is for the shock-free branch. Inclusion of an opacity factor (which reduces photo-dissociation) shifts the burning towards the black hole. The disk is found to be completely stable even in presence of nucleosynthesis.

Case B.2: As discussed in Sect. 2, in extreme hard states, a black hole may accrete very little matter in the Keplerian component and very large amount of matter in the sub-Keplerian component. To simulate this we used B.1 parameters, but $\dot{m} = 4$. The resulting solution is found to be unstable when shocks are present. In Fig. 5b, we superimposed velocity variation without nuclear energy (same as with nuclear energy as far as Case B.1 is concerned) and with nuclear energy. The dash-dotted curve next to the un-shocked branch and dashed curve next to the shocked branch show the resulting deviation. While the branch without shock still remains stable, the other branch is distinctly unstable as the steady-state solution is sub-sonic at the inner edge. The only solution available must be non-steady with oscillations near the sonic point.

Case B.3: In this case, accretion rate is chosen to be even smaller ($\dot{m} = 0.001$) and the polytropic index is chosen to be 5/3. The maximum temperature reaches $T_9^{\mathrm{max}} = 47$. After leaving the Keplerian flow, the temperature and velocity of the flow monotonically increases. Because of excessive temperature, D and ^{3}He are photo-dissociated immediately after the flow leaves the Keplerian disk at $x_K = 84.4$. At around $x = 30$, all ^{4}He is photo-dissociated exactly as in Case B.1. Subsequently, the flow contains only protons and neutrons and there is no more energy release from the nuclear reactions. This behaviour is clearly seen in Fig. 6. The notations are the same as in the previous run. This ultra-hot case is found to be stable since the energy release took place far away from the black hole where the matter was moving slowly and therefore the rate (Q_{nuc}) was not high compared to that due to viscous dissipation (units are as Fig. 2d).
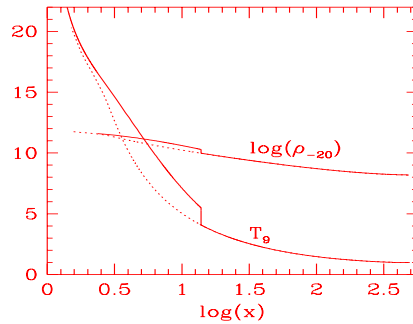

Fig. 5a

Case B.4: In this case, the net accretion rate is low ($\dot{m} = 0.01$) but viscosity is high and the efficiency of emission is intermediate ($f = 0.2$). That means that the temperature of the flow is high ($F_{\mathrm{Compt}} = 0.1$, maximum temperature $T_9^{\mathrm{max}} = 13$). Matter deviates from a Keplerian disk at around $x_K = 8.4$. Assuming that the high viscosity is due to stochastic magnetic field, protons would be drifted towards the black hole due to magnetic viscosity, but the neutrons will not be drifted (Rees et al. 1982). They will generally circle around the black hole till they decay. This principle has been used to do the simulation in this case. The modified composition in one sweep is allowed to interact with freshly
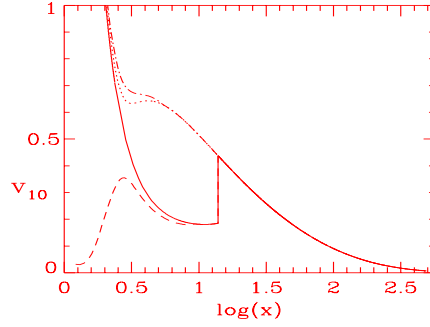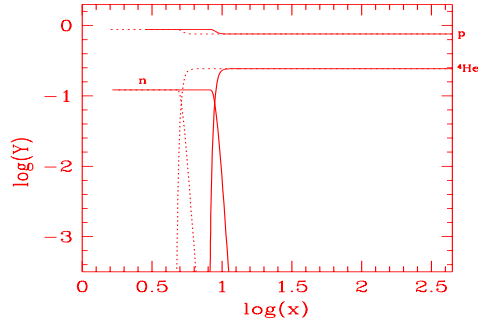
Fig. 5b

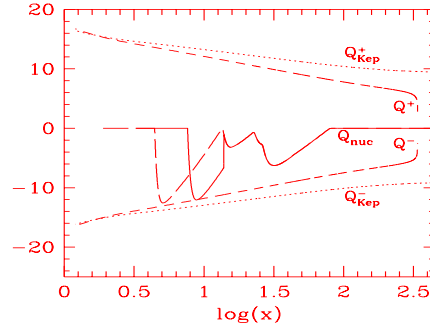**Fig. 5c**

Fig. 5d

Fig. 5. Variation of (a) ion temperature (T_9) and density (ρ_{-20}), (b) radial velocity v_{10}, (c) matter abundance Y_i in logarithmic scale and (d) various forms of height-integrated specific energy release and absorption rates when the model parameters are $M = 10M_\odot$, $\dot{m} = 0.01$, $\alpha_\Pi = 0.05$ as functions of logarithmic radial distance (x in units of Schwarzschild radius). See text and Table 1 for other parameters of Case B.1 which is considered here. Solutions in the stable branch with shocks are solid curves and those without the shock are short dashed in (a-c). Curves in (d) are described in the text. The ultra-hot temperature of the flow photo-dissociates ^4He into protons and neutrons. The shocked branch (which is stable) causes such dissociation farther out from the black hole than the unstable shock-free branch. In (b), dot-dashed curve and dashed curves are drawn when nuclear energy is taken into account and $\dot{m} = 4$ is chosen (Case B.2).

accreting matter with the understanding that the accumulated neutrons do not drift radially. After few iterations or sweeps the steady distribution of the composition is achieved. Figure 7 shows the neutron distribution in the sub-Keplerian region. The formation of a 'neutron torus' is very apparent in this result. In fact, the formation of a neutron disk is very generic in all the hot, highly viscous accretion flows as also seen in Cases B.1-B.3 (for details, see, Paper 1). The nuclear reactions leading to the neutron torus formation are exactly same as previous cases and are not described here.
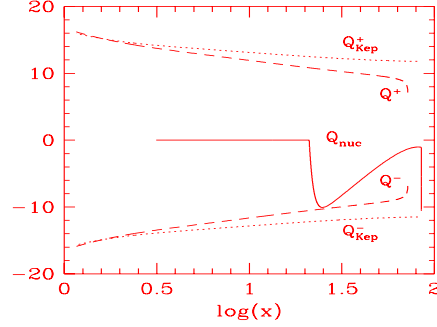
Fig. 6. Specific nuclear energy rate variation curve (solid) for a $\gamma = 5/3$, ultra-hot case ($T_9^{\mathrm{max}} = 44$) as functions of logarithmic radial distance (x in units of Schwarzschild radius). The entire initial abundance is photo-dissociated at $x \gtrsim 30$. The viscous energy generation curve (Q^+) and absorption curve (Q^-) [both long dashed] are presented for comparison. $Q_{\mathrm{Kep}}^{\pm}$ (dotted) curves are the specific energy generation and absorption rates provided the inner disks were Keplerian. Qs are in units of ergs cm^{-2} sec^{-1}. See Table 1 for parameters of Case B.3.
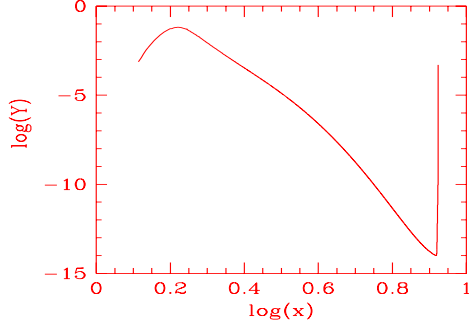

Fig. 7

Fig. 7. Formation of a *neutron torus* in a hot inflow. Neutron abundance as a function of the logarithmic radial distance (x in units of Schwarzschild radius). See, Table 1 for parameters of Case B.4.

3.3. Nucleosynthesis in Cooler Flows

Case C.1: Here we choose a high-viscosity flow with a very high accretion rate. Matter deviates from the Keplerian disk very close to the black hole $x_K = 4.8$. The flow in the centrifugal barrier is cooler (temperature maximum $T_9^{\mathrm{max}} = 0.8$). Here clearly, high viscosity removes the centrifugal barrier completely and matter falls in almost freely. Due to very short residence time, no significant change in the composition takes place. Only a small amount of proton capture (mainly due to $^{11}B(p,\gamma)3^4He$, $^{16}O(p,\alpha)^{13}N$, $^{15}N(p,\alpha)^{12}C$, $^{18}O(p,\alpha)^{15}N$, $^{19}F(p,\alpha)^{16}O$) takes place. A small amount of deuterium dissociation also take place, but it does not change the energetics significantly. The flow is not found to be unstable in this case.

Case C.2: This is a test case for the proto-galactic accretion flow. In the early phase of galaxy formation, the supply of matter is high, and the temperature of the flow is very low. The viscosity may or may not be very high, but we choose very low (presumably, radiative) viscosity ($\alpha = 10^{-4}$). The motivation is to use similar parameters as were used in JAC while studying the nucleosynthesis in thick accretion disks. The central mass $M = 10^6 M_\odot$, the maximum

temperature is $T_9^{\max} \sim 0.2$ and the Comptonization factor $F_{Compt} = 0.001$. The temperature variation is similar to Fig. 2a when scaled down by a factor of 30 (basically by the ratio of the F_{Compt} values). The velocity variation is similar to Fig. 2b and is not repeated here. Due to the low temperature, there is no significant change in the nuclear abundance. Note that since thick accretion disks are rotation dominated, the residence time was very long in CJA simulation and there *was* significant change in composition even at lower temperatures. But in this case the flow radial velocity is very high and the residence time is shorter. The nuclear energy release is negligible throughout and is not shown.

4. Nucleosynthesis Induced Instability

CJA, while studying nucleosynthesis in cooler, mainly rotating disks, suggested that as long as the nuclear energy release is smaller than the gravitational energy release, the disk would be stable. In the present paper, we find that this suggestion is still valid. Indeed, even when momentarily the nuclear energy release or absorption is as high as the gravitational energy release (through viscous dissipation), the disk may be stable. For instance, in case A.1 (Fig. 2d) at around $x = 4$ these rates are similar. Yet the velocity, temperature and density distributions (Fig. 2a-b) remain unchanged. In Case A.3, Q_{nuc} is several magnitudes greater than viscous energy release Q^+ and the thermodynamic quantities are indeed disturbed to the extent that the flow with same injected quantities (with the same density and velocity and their gradients) at the outer edge does not become supersonic at the inner edge. In these cases, the flow must be unsteady in an effort to search for the 'right' sonic point to enter into the black hole. On the other hand, ultra-hot cases like B.2 show deviation in non-shocked solution while the shocked solution is unstable.

The general behaviour suggests that the present model of accretion disks is more stable under nuclear reactions compared to the earlier, predominantly rotating model. Here, the radial velocity (v) spreads energy release or absorption radially to a distance $v\tau_D(\rho, T) = vN_D/\dot{N}_D$ cm, where, N_D is the number density of, say, Deuterium and $\dot{N}_D$ is its depletion rate. For a free fall, $v \sim x^{-1/2}$, while for most nuclear reactions, $\tau_D(\rho, T) \sim x^n$, with $n >> 1$ (since reaction rates are strongly dependent on density and temperature). Thus, Q_{nuc} for the destruction of a given element spreads out farther away from the black hole, but steepens closer to it. Large dQ_{nuc}/dx causes instability since the derivatives such as dv/dx at the inner regions (including the sonic point) become imaginary.

5. Discussions and Conclusions

In this paper, we have explored the possibility of nuclear reactions in inner accretion flows. Because of high radial motion and ion pressure, matter deviates from a Keplerian disk close to the black hole. The temperature in this region is controlled by the efficiencies of bremsstrahlung and Comptonization processes (CT96, C97) and possible heating by magnetic fields (Shapiro 1973): for a higher Keplerian rate and higher viscosity, the inner edge of the Keplerian component comes closer to the black hole and the sub-Keplerian region becomes cooler (CT95). The nucleosynthesis in this soft state of the black hole is quite negligible. However, as the viscosity is decreased to around 0.05 or less, the inner edge of the Keplerian component moves away and the Compton cooling becomes less efficient due to the paucity of the supply of soft photons. The sub-Keplerian region, though cooler by a factor of about $F_{\mathrm{Compt}} = 0.01$ to 0.03 from that of the value obtained through purely hydrodynamical calculations of C96, is still high enough to cause significant nuclear reactions to modify compositions. The composition changes very close to the black hole, especially in the centrifugal-pressure-supported denser region, where matter is hotter and slower.

The degree of change in compositions which takes place in the Group A and B calculations, is very interesting and its importance must not be underestimated. Since the centrifugal-pressure-supported region can be treated as an effective surface of the black hole which may generate winds and outflows in the same way as the stellar surface (Chakrabarti 1998a,b; Das & Chakrabarti 1999), one could envisage that the winds produced in this region would carry away a modified composition and contaminate the atmosphere of the surrounding stars and the galaxy in general.

One could estimate the contamination of the galactic metalicity due to nuclear reactions. For instance, in Case A.1, ^{12}C, ^{16}O, ^{20}Ne, ^{30}Si, ^{44}Ca and ^{52}Cr are found to be over-abundant in some region of the disk. Assume that, on an average, all the N stellar black holes are of equal mass M and have a non-dimensional accretion rate of around $\dot{m} \sim 1$ ($\dot{m} = \dot{M}/\dot{M}_{\mathrm{Edd}}$). Let ΔY_i (few times 10^{-3}) be the typical change in composition of this matter during the run and let f_w be the fraction of the incoming flow that goes out as winds and outflows (could be from ten percent to more than a hundred percent when disk evacuation occurs), then in the lifetime of a galaxy (say, 10^{10}yrs), the total 'change' in abundance of a particular species deposited in the surroundings by all the stellar black holes is given by:

$$< \Delta Y_i >_{\mathrm{small}} \cong 10^{-7}(\frac{\dot{m}}{1})(\frac{N}{10^6})(\frac{\Delta Y_i}{10^{-3}})(\frac{f_w}{0.1})(\frac{M}{10 M_\odot})(\frac{T_{\mathrm{gal}}}{10^{10}} Yr)(\frac{M_{\mathrm{gal}}}{10^{11} M_\odot})^{-1}. \qquad (2)$$

The subscript 'small' is used here to represent the contribution from small black holes. We also assume a conservative estimate that there are 10^6 such stellar black holes in a galaxy, the mass of the host galaxy is around $10^{11} M_\odot$ and the lifetime of the galaxy during which such reactions are going on is about 10^{10}Yrs. We also assume that $\Delta Y_i \sim 10^{-3}$ and a fraction of ten percent of matter is blown off as winds. The resulting $< \Delta Y_i > \sim 10^{-7}$ may not be very significant if one considers averaging over the whole galaxy. However, for a lighter galaxy $< \Delta Y_i >$ could be much higher. For example, for $M_{gal} = 10^9 M_\odot$, $< \Delta Y_i > \sim 10^{-5}$. This would significantly change the average abundances of ^{30}Si, ^{44}Ca and ^{52}Cr. On the other hand, if one concentrates on the region of the outflows only, the change in abundance is the same as in the disk, and should be detectable (e.g., through line emissions). One such observation of stronger iron-line emission was reported for SS433 (Lamb et al. 1983; see also Arnould & Takahashi 1999, for a recent discussion on galactic contaminations).

When we consider a case like A.3, we find that ^{12}C, ^{16}O, ^{20}Ne, and ^{28}Si are increased by about 10^{-3} in some regions. In this case, the average change of abundance due to accretion onto the massive black hole situated at the galactic centre would be,

$$< \Delta Y_i >_{\text{big}} \cong few \times 10^{-8} (\frac{\dot{m}}{1})(\frac{\Delta Y_i}{10^{-3}})(\frac{f_w}{0.1})(\frac{M}{10^6 M_\odot})(\frac{T_{\text{gal}}}{10^{10}} Yr)(\frac{M_{\text{gal}}}{10^{11} M_\odot})^{-1}. \tag{3}$$

Here, we have put 'big' as the subscript to indicate the contribution from the massive black hole. Even for a lighter galaxy, e.g., of mass $M_{\text{gal}} = 10^9 M_\odot$, $\Delta Y_i = 10^{-6}$ which may not be significant. If one considers only the regions of outflows, contamination may not be negligible.

A few related questions have been asked lately: Can lithium be produced in black hole accretion? We believe not. The spalletion reactions (Jin 1990; Yi & Narayan 1997) which may produce such elements assuming that a helium beam hits a helium target in a disk. Using a full network, rather than only He-He reaction, we find that the hotter disks where spalletion would have been important also photo-dissociate (particularly due to the presence of photons from the Keplerian disk) helium to deuterium and then to protons and neutrons before any significant lithium could be produced. Even when photo-dissociation is very low (when the Keplerian disk is far away, for instance), or when late-type stellar composition is taken as the initial composition, we find that the ^7Li production is insignificant, particularly if one considers more massive black holes ($M \sim 10^8 M_\odot$).

Recently, it has been reported by several authors (Martin et al. 1992; 1994; Fillipenko et al. 1995; Harlaftis et al. 1996) that a high abundance of Li is observed in late type stars which are also companions of black hole and neutron star candidates. This is indeed surprising since the theory of stellar evolution predicts that these stars should have at least a factor of ten lower Li abundance. These workers have suggested that this excess Li could be produced in the hot accretion disks. However, in Paper 1 as well as in our Cases A and B computations we showed that Li is not likely to be produced in accretion disks. Indeed, we ran several cases with a mass fraction of He as high as 0.5 to 0.98, but we are still unable to produce Li with a mass fraction more than 10^{-10}. Recent work of Guessoum & Kazanas (1999) agrees with our conclusion that profuse neutrons would be produced in the disk. They farther suggested that these energetic neutrons can produce adequate Li through spalletion reactions with the C, N, and O that is present in the atmospheres of these stars. For instance, in Cases B.1 and B.3 we see that neutrons could have an abundance of ~ 0.1 in the disk. Since the production rate is similar to what Guessoum & Kazanas (1999) found, Li should also be produced on stellar surface at a similar rate.

What would be the neutrino flux on earth if nucleosynthesis does take place? The energy release by neutrinos (the pair neutrino process, the photoneutrino process and the plasma neutrino process) can be calculated using the prescription of Beaudet et al. (1967, hereafter BPS; see also Itoh et al. 1996) provided the pairs are in equilibrium with the radiation field. However, in the case of accretion disks, the situation is significantly different from that inside a star (where matter is in static equilibrium). Because of rapid infall, matter density is much lower and the infall time scale could be much shorter compared to the time-scale of various neutrino processes, especially the pair and photo-neutrino processes. As a result, the pair density need not attain equilibrium. One important thing in this context is the opacity (τ_{pair}) of the pair process. Following treatments of Colpi et al. (1984) we find that $\tau_{\text{pair}} < 1$ for all our cases, and therefore pair process is expected to be negligible (for Case B.2, τ_{pair} is the highest [0.9]). Park (1990a,b), while studying pair creation processes in spherical accretion, shows that even in the most favourable condition, the ratio of positron (n_+) and ion (n_i) is no more than 0.05. A simple analysis suggests that neutrino production rate is many orders of magnitude smaller compared to what the equilibrium solutions of BPS and Itoh et al. would predict. Thus, we can safely ignore the neutrino luminosity.

When the nuclear energy release or absorption is comparable to the gravitational energy release through viscous processes, we find that the disk is still stable. Stability seems to depend on how steeply the energy is released or absorbed in the disk. This in turn depends on $\tau_D v$, the distance traversed inside the disk by the element contributing the highest change of energy before depleting significantly. Thus, an ultra-hot case (Group B) can be stable even

though a hot (Group A) case can be unstable as we explicitly showed by including nuclear energy release. In these 'unstable' cases, we find that the steady flow does not satisfy the inner boundary condition and becomes subsonic close to the horizon. This implies that in these cases the flow must become non-steady, constantly searching for the supersonic branch to enter into the black hole. This can induce oscillations as have been found elsewhere (Ryu et al. 1997). In such cases, one is required to do time dependent simulations (e.g., Molteni et al. 1994, 1996) to include nuclear reactions. This will be attempted in future.

References

Anders E., Ebihara M., 1982, Geochim. Cosmochim. Acta 46, 2363
Arai K., Hashimoto M., 1992, A&A 254, 191
Arnett W.D., Truran J., 1969, ApJ 157, 339
Arnould M., Takahashi K., 1999, Rep. Prog. Phys. 62, 395
Beaudet G., Petrosian V., Salpeter E.E., 1967, ApJ 150, 979 (BPS)
Chakrabarti S.K., 1986, in Accretion Processes in Astrophysics, Audouze J., Tran Thanh Van, J., (eds.) Editions Frontières: Paris, p.155
Chakrabarti S.K., 1990, Theory of Transonic Astrophysical Flows, Singapore: World Scientific
Chakrabarti S.K., 1996, ApJ 464, 623 (C96)
Chakrabarti S.K., 1997, ApJ 484, 313 (C97)
Chakrabarti S.K., 1998a, Ind. J. Phys. 72(B), 183
Chakrabarti S.K., 1998b, In: Observational Evidence for Black Holes in the Universe, Chakrabarti S.K. (ed.), Kluwer Academic Publishers, Dordrecht, p. 19
Chakrabarti S.K., Jin L., Arnett W.D., 1987, ApJ 313, 674 (CJA)
Chakrabarti S.K., Molteni D., 1993, ApJ 417, 671
Chakrabarti S.K., Molteni D., 1995, MNRAS 272, 80
Chakrabarti S.K., Mukhopadhyay B., 1999, A&A 344, 105 (Paper 1)
Chakrabarti S.K., Titarchuk L., 1995, ApJ 455, 623 (CT95)
Colpi M., Maraschi L., Treves A., 1984, ApJ 280, 319
Das T.K. & Chakrabarti, S.K. 1999, Class. Quantum Grav. (in press).
Filippenko A.V., Matheson T., Barth A.J., 1995, ApJ 455, L139
Fowler W.A., Caughlan G.R. , Zimmerman B.A., 1975, ARA&A 13, 69
Fuller G.M., Fowler W.A., Newmann M.J., 1980, ApJS 42, 447
Fuller G.M., Fowler W.A., Newmann M.J., 1982, ApJS 48, 279
Gilfanov M., Churazov E., Sunyaev R.A., 1997, in Accretion Disks – New Aspects, Meyer-Hofmeister E., Spruit H. (eds.), Springer (Heidelberg).
Guessoum N., Kazanas D., 1999, ApJ 512, 332
Harlaftis E.T., Horne K., Filippenko, A.V., 1996, PASP 168, 762
Harris M.J., Fowler W.A., Caughlan G.R., Zimmerman, B.A., 1983, ARA&A 21, 165
Hashimoto M., Eriguchi Y., Arai K., Müller E., 1993, A&A 268, 131
Hawley J.W., Smarr L.L., Wilson J.R., 1984, ApJ 277, 296
Hawley J.F., Smarr L.L., Wilson J.R., 1985, ApJS 55, 211
Itoh N., Hayashi H., Nishikawa A., Kohyama Y., 1996, ApJS 102, 411
Jin L., 1990, ApJ 356, 501
Jin L., Arnett W.D., Chakrabarti S.K., 1989, ApJ 336, 572 (JAC)
Lamb R.C. , Ling J.C., Mahoney W.A. et al., 1983, Nat 305, 37
Lu J.F., Yuan F., 1997, PASJ 49, 525
Lu J.F., Yu K.N., Yuan F., Young E.C.M., 1997, A&A 321, 665
Martin E.L., Rebolo R., Casares J., Charles P.A., 1992, Nat 358, 129
Martin E.L., Rebolo R., Casares J., Charles P.A., 1994, ApJ 791, 435
Molteni D., Lanzafame G., Chakrabarti S.K., 1994, ApJ 425, 161
Molteni D., Ryu D., Chakrabarti S.K., 1996, ApJ 470, 460
Nobuta K., Hanawa T., 1994, PASJ 46, 257
Park M., 1990a, ApJ 354, 64
Park M., 1990b, ApJ 354, 83
Rees, M.J., 1984, ARA&A 22, 471
Rees M.J., Begelman M.C., Blandford R.D., Phinney E.S., 1982, Nat 295, 17
Ryu D., Brown J.G.L., Ostriker J.P., Loeb A., 1995, ApJ 452, 364
Ryu D., Chakrabarti S.K., Molteni D., 1997, ApJ 474, 378

Shakura N.I., Sunyaev R.A., 1973, A&A 24, 337
Shapiro S.L., 1973, ApJ 180, 531
Shvartsman V.F., 1971, Sov. Astron. A.J. 15, 377
Sponholz H., Molteni D., 1994, MNRAS 271, 233
Thielemann F.-K., 1980, Ph.D. Thesis, Max Planck Institut, Munich and Technische Hochschule, Darmstadt
Wagoner R., Fowler W.A., Hoyle F., 1967, ApJ 148, 3
Wallace R.K., Woosley S.E., 1981, ApJS 231, 26
Woosley S.E., Arnett W.D., Clayton D.D., 1973, ApJS 231, 26
Yang R., Kafatos M., 1995, A&A 295, 238
Yi I., Narayan R., 1997, ApJ 486, 38
Zhang S.N., Ebisawa K., Sunyaev R., et al., 1997, ApJ 479, 381